

Dynamic Lattice Distortions in Sr_2RuO_4 : A microscopic study by perturbed angular correlation (TDPAC) spectroscopy

S.N. Mishra*

Department of Nuclear and Atomic Physics, Tata Institute of Fundamental Research, Homi Bhabha Road, Mumbai-400005, India

M. Rots and S. Cottenier[†]

Instituut voor Kern- en Stralingsfysica and INPAC, Katholieke Universiteit Leuven, Celestijnenlaan 200 D, BE-3001 Leuven, Belgium

(Dated: April 24, 2017)

Applying time differential perturbed angular correlation (TDPAC) spectroscopy and *ab initio* calculations, we have investigated possible lattice instabilities in Sr_2RuO_4 by studying the electric quadrupole interaction of a ^{111}Cd probe at the Ru site. We find evidence for a dynamic lattice distortion, revealed from the observations of: (i) a rapidly fluctuating electric-field gradient (EFG) tensor of which the main component decreases with decreasing temperature, and (ii) a monotonic increase of the EFG asymmetry (η) below 300 K. We argue that the observed dynamic lattice distortion is caused by strong spin fluctuations associated with the inherent magnetic instability of Sr_2RuO_4 .

PACS numbers: 71.27.+a, 74.70.Pq, 76.80.+y, 71.15.Mb

I. INTRODUCTION

Since the discovery of unconventional superconductivity in the non-cuprate oxide Sr_2RuO_4 , considerable attention has been paid to study its electronic and magnetic properties in the normal and superconducting states.^{1,2} This material – with a layered perovskite structure identical to the prototype high- T_c superconductor $(\text{La}, \text{Sr}/\text{Ba})_2\text{CuO}_4$ – has been identified to exhibit spin triplet (p-wave) superconductivity below 1 K.^{1,2} Besides superconductivity, Sr_2RuO_4 exhibits several other unusual features in its normal state. For instance, transport studies have revealed Fermi liquid behavior with an electrical resistivity that shows quadratic temperature dependence below 25 K.³ Secondly, the material shows a large electronic specific heat ($\gamma \approx 37.5$ mJ/mol-K²) and a strongly enhanced Pauli susceptibility ($\chi_0 \approx 9 \times 10^{-4}$ emu/mol) reflecting heavy-fermion behavior.^{3,4} It has been recognized that both structural and magnetic instabilities play a crucial role for the unconventional superconductivity in Sr_2RuO_4 .^{1,5} Recent theoretical calculations have suggested that Sr_2RuO_4 is close to a ferromagnetic (FM) instability^{6,7} with strong FM spin fluctuations which may lead to spin triplet p-wave superconductivity.⁸

As for the structural aspect, while crystal transformation is common in most cuprate oxides, no long range structural distortion/transformation has been detected for Sr_2RuO_4 down to 100 mK.^{9,10,11} However, a local (short-ranged) structural instability related to a rotation of the RuO_6 octahedra has been detected by Braden et al., using phonon dispersion information obtained by inelastic neutron scattering.¹² To our knowledge, no other experimental study related to structural instabilities in Sr_2RuO_4 has been reported. Considering the many unusual physical properties, including unconventional superconductivity, it is desirable to carry

out additional investigations, particularly with help of microscopic techniques, to examine structural distortions/instabilities in undoped Sr_2RuO_4 . For this purpose, hyperfine methods such as Mössbauer spectroscopy, Nuclear Magnetic/Quadrupole Resonance (NMR/NQR) or Time-Differential Perturbed Angular Correlation (TDPAC) are extremely useful. In particular, information on structural properties such as lattice transformation and/or distortion can be extracted by studying the electric-field gradient (EFG) tensor obtained from nuclear quadrupole interaction measurements. Performing such studies with NMR or NQR has been found to be difficult, due to a.o. low isotopic abundance, small quadrupole moments, strong spin lattice relaxation and large line broadening.^{13,14,15} Similarly, due to the large line width, Mössbauer spectroscopy using the native ^{99}Ru isotope is also not suitable for measuring small lattice distortions. Such experimental difficulties, however, can be overcome using the TDPAC method¹⁶. With a suitable probe nucleus such as ^{111}Cd , the TDPAC technique can be very effective for detection of static and dynamic lattice distortions.

In this paper we report our results on a lattice instability in Sr_2RuO_4 observed from quadrupole interaction measurements at a ^{111}Cd probe nucleus measured by TDPAC spectroscopy. The experimental results show evidence of a *dynamic* lattice distortion below 300 K revealed by: (i) a rapidly fluctuating electric-field gradient (EFG) tensor and (ii) a temperature dependent change of the EFG asymmetry parameter η . Taking into account *ab initio* calculations based on Density Functional Theory (DFT), we argue that the observed dynamic lattice distortion is caused by strong spin fluctuations associated with an inherent magnetic instability of Sr_2RuO_4 .

II. EXPERIMENTAL AND COMPUTATIONAL DETAILS

A polycrystalline sample of Sr_2RuO_4 was prepared following a standard procedure. A mixture of stoichiometric amounts of high purity SrCO_3 and RuO_2 was pelletized and sintered at 1100°C for 12 h. After regrinding, the powder was pressed into a pellet and heated in air at 1100°C for another 18 h followed by furnace cooling. The sample was characterized by powder X-ray diffraction, showing a single phase having the K_2NiF_4 -type tetragonal structure with lattice parameters $a = 3.868(5) \text{ \AA}$ and $c = 12.732(5) \text{ \AA}$ which agree well with the earlier data.^{3,9,10,11} The ^{111}Cd probe was introduced into a small piece of Sr_2RuO_4 by diffusing carrier free parent ^{111}In activity at 1050°C for 24 h followed by rapid cooling to room temperature. It is important to mention that the typical concentration of Cd in the sample remains below 1 ppm and thus does not alter the basic physical properties of the material. The electric quadrupole interaction parameters were extracted from the life time spectra of the 247 keV, $I=5/2$ and 84 ns level of the daughter ^{111}Cd nucleus produced by electron capture (EC) decay of ^{111}In . The time spectra were recorded simultaneously in a $90^\circ/180^\circ$ geometry using a set-up consisting of four BaF_2 detectors and a standard slow-fast coincidence circuit having a time resolution better than 700 ps. Measurements were carried out as a function of temperature in the range 20-500 K using either a closed cycle helium refrigerator or a specially designed furnace. The perturbation factor $A_{22}G_{22}(t)$ in the angular correlation function $W(\theta, t) = \sum_{kk} A_{kk}G_{kk}(t)P_k(\cos\theta)$ was obtained by constructing the appropriate ratio function, called the TDPAC time spectrum¹⁶,

$$R(t) = A_{22}G_{22}(t) = \frac{2[W(180^\circ, t) - W(90^\circ, t)]}{[W(180^\circ, t) + 2W(90^\circ, t)]}$$

where $W(\theta, t)$ are the background-subtracted normalized coincidence counts of detectors placed at 180° and 90° . The spectra were fitted to the function¹⁶

$$A_{22}G_{22}(t) = \frac{A_{22}}{5} \left[1 + \sum_{n=1}^3 S_n(\eta) e^{-nt/\tau_N} \cos(n\omega_0(\eta)t) \right]$$

to extract the interaction frequency ω_0 related to the principal component V_{zz} of the EFG tensor¹⁶:

$$\omega_0 = \frac{6eQV_{zz}}{\hbar 4I(2I-1)} \quad (1)$$

(expression valid for half-integer spin), the asymmetry $\eta = V_{xx} - V_{yy}/V_{zz}$ of the EFG tensor, and the relaxation time τ_N which is related to the distribution width δ of ω_0 by $\tau_N = 1/\delta$. For our data, using a Lorentzian frequency distribution yielded a better χ^2 than a Gaussian spread in ω_0 .

TABLE I: Comparison of some structural and electric-field gradient parameters for $I4/mmm$ Sr_2RuO_4 with fully optimized theoretical lattice constants and internal positions (left), and the corresponding experimental data (right).

	theory	experiment
$a=b$ (\AA)	3.8937	3.862 [10]
c (\AA)	12.8935	12.722 [10]
z_{Sr}	0.3525	0.3534 [10]
$z_{\text{O}(2)}$	0.1626	0.1613 [10]
$d_{\text{Sr-Ru}}$ (\AA)	3.3464	3.3069 [10]
$d_{\text{Ru-O}(2)}$ (\AA)	2.0962	2.0521 [10]
V_{zz} Sr (10^{21} V/m^2)	-2.42	-
V_{zz} Ru (10^{21} V/m^2)	-0.99	± 2.05 [15]
V_{zz} O(1) (10^{21} V/m^2)	+7.90	± 8.1 [13]
V_{zz} O(2) (10^{21} V/m^2)	+7.10	± 6.4 [13]
η O(1)	0.265	0.17 [13]

Complimentary to the TDPAC experiments, we performed a series of *ab initio* calculations on pure and Cd-doped Sr_2RuO_4 . The calculations were performed within Density Functional theory^{22,23,24}, using the Augmented Plane Waves + local orbitals (APW+lo) method^{24,25,26} as implemented in the WIEN2k package²⁷ to solve the scalar-relativistic Kohn-Sham equations. In the APW+lo method, the wave functions are expanded in spherical harmonics inside nonoverlapping atomic spheres of radius R_{MT} , and in plane waves in the remaining space of the unit cell (=the interstitial region). For Sr, Ru and Cd a R_{MT} value of 1.85 a.u. was chosen, for O we used $R_{\text{MT}}=1.55$ a.u. The maximum ℓ for the expansion of the wave function in spherical harmonics inside the spheres was taken to be $\ell_{\text{max}} = 10$. The plane wave expansion of the wave function in the interstitial region was made up to $K_{\text{max}} = 7.5/R_{\text{MT}}^{\text{min}} = 4.83 \text{ a.u.}^{-1}$ for pure Sr_2RuO_4 and for supercells with 8 formula units, and up to $K_{\text{max}} = 5.75/R_{\text{MT}}^{\text{min}} = 3.71 \text{ a.u.}^{-1}$ for supercells with 16 formula units (this reduced accuracy has an effect on e.g. the electric-field gradient of less than 10%). The charge density was Fourier expanded up to $G_{\text{max}} = 16\sqrt{Ry}$. For the sampling of the Brillouin zone, a special k-mesh equivalent to $8 \times 8 \times 8$ mesh in the pure Sr_2RuO_4 structure was used throughout. As exchange-correlation functional, the Perdew-Burke-Ernzerhof Generalized Gradient Approximation (GGA) was used.²⁸ As Table I shows, this type of calculations is able to reproduce correctly some experimentally known structural and EFG properties of pure Sr_2RuO_4 . The structural information is also in agreement with previous *ab initio* calculations,²⁹ while for the EFG's our GGA results show much better agreement with respect to experiment than reported values obtained using the Local Density Approximation.³⁰

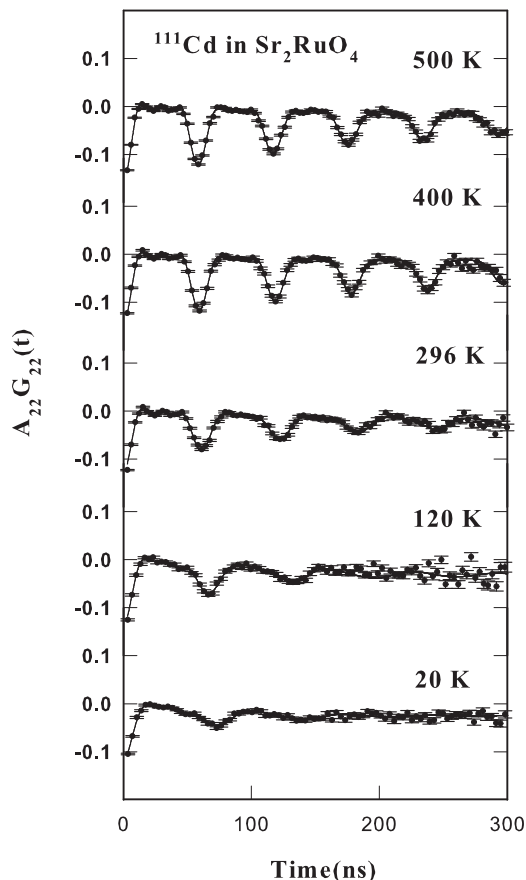


FIG. 1: Typical TDPAC spectra for ^{111}Cd in Sr_2RuO_4 at different temperatures.

III. RESULTS AND DISCUSSION

Figure 1 shows some typical TDPAC spectra of ^{111}Cd in Sr_2RuO_4 at different temperatures. All spectra show a single quadrupole interaction frequency with nearly the full anisotropy ($A_{22} \approx 0.13$), indicating that the ^{111}Cd probe atoms occupy a unique lattice site. From a comparison of the chemical behaviour and ionic size of the mother isotope ^{111}In and the atomic species of the sample under investigation, the Cd probe atoms are likely to occupy a substitutional Ru site in Sr_2RuO_4 . This assignment of lattice site is supported by earlier TDPAC results in related materials, e.g. SrRuO_3 and CaRuO_3 ¹⁷ where Cd has been reported to appear at the Ru site, and is corroborated by the EFG-values found from our *ab initio* calculations (see Tab. III and the corresponding discussion). The spectra recorded above 300 K could be simulated with a single randomly oriented, axially symmetric ($\eta=0$) electric-field gradient (EFG). From Eq. 1 and using the experimental quadrupole moment $Q = 0.83 \text{ b}^{18}$, the principal component of the EFG at room temper-

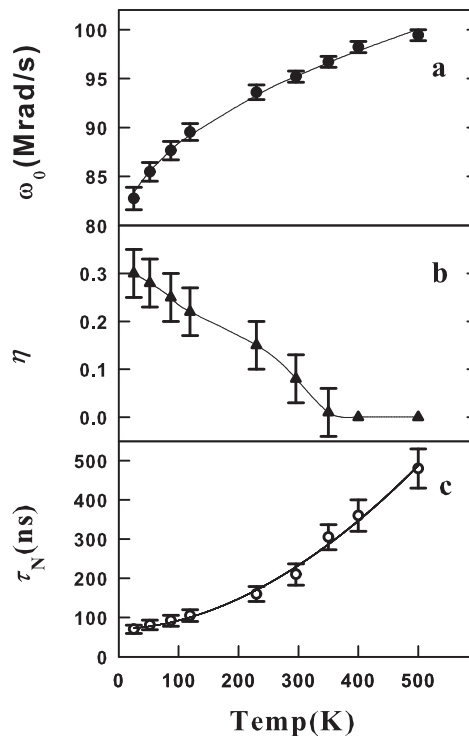


FIG. 2: Temperature dependence of the quadrupole interaction frequency (ω_0), electric field gradient asymmetry parameter (η), and the nuclear relaxation time (τ_N) measured for ^{111}Cd in Sr_2RuO_4 . The solid line in (b) is a guide to the eye whereas in (a) and (c) they correspond to least square fits to equations discussed in the text.

ature was determined to be $V_{zz} = 5.2(1) \times 10^{21} \text{ V/m}^2$. Below 300 K the TDPAC spectra show a noticeable deviation from the axially symmetric quadrupole interaction patterns observed at higher temperatures (Fig. 1). They could be fitted with a randomly oriented, asymmetric EFG yielding $\omega_0 = 82.7(11) \text{ Mrad/s}$ and asymmetry parameter $\eta=0.30(3)$ at 20 K. In addition, the observed $R(t)$ spectra show temperature dependent damping, most pronounced at low temperatures (see Fig. 1). Fig. 2 displays the variation of ω_0 , η and the relaxation time $\tau_N = 1/\delta(\omega_0)$ as a function of temperature (see also Table II). The relaxation time τ_N measures the spread in interaction frequencies, and therefore is an indication of the number of different environments felt by the probe nucleus.

The TDPAC results obtained for ^{111}Cd in Sr_2RuO_4 (Fig. 2 and Table II) reveal several interesting features. First of all, the quadrupole interaction frequency ω_0 increases from 82.7(11) Mrad/s at 20 K to almost 100 Mrad/s at 500 K. This variation of ω_0 as a function of temperature could be parameterized using the relation

$$\omega_0(T) = \omega_0(0)(1 + AT^\alpha)$$

TABLE II: Summary of quadrupole interaction parameters for ^{111}Cd in Sr_2RuO_4 .

Temperature (K)	ω_0 (Mrad/s)	V_{zz} ($10^{21}\text{V}/\text{m}^2$)	η	τ_N (ns)
20	82.7(9)	4.56(10)	0.30(5)	70(20)
52	85.5(8)	4.71(10)	0.27(5)	81(20)
87	87.7(7)	4.84(10)	0.25(5)	95(20)
119	90.0(5)	4.97(10)	0.22(5)	115(20)
230	94.0(3)	5.03(10)	0.15(5)	170(25)
296	95.2(3)	5.20(10)	0.08(5)	220(35)
350	96.7(2)	5.11(10)	0.0	310(40)
400	98.2(2)	5.19(10)	0.0	380(50)
500	99.5(2)	5.26(10)	0.0	480(60)

with $\omega_0(T = 0) = 77.8(14)$ Mrad/s (or $V_{zz}(T = 0) = 4.2 \times 10^{21}$ V/m²), $A = 0.016(5)$ and $\alpha = 0.47(6)$. Considering that Sr_2RuO_4 is a metallic system^{1,2}, the quadrupole interaction frequency is expected to *decrease* with increasing temperature, following a $T^{3/2}$ law due to lattice vibrations.^{19,20} Instead, the ω_0 measured for ^{111}Cd in Sr_2RuO_4 *increases* with temperature and approximately shows a \sqrt{T} dependence.

Secondly, while the EFG is observed to be axially symmetric above 300 K ($\eta = 0$), it shows a significant amount of asymmetry at low temperatures with $\eta(T)$ monotonically increasing up to ≈ 0.3 at 20 K. These observed $\eta(T)$ data provide a direct proof that i) the local site symmetry of the Cd probe atom is *not* cubic as expected for the Ru site in this lattice structure, and ii) continuously changes below 300 K.

Thirdly, the relaxation time τ_N extracted from the damping of the R(t) spectra strongly varies with temperature (Fig. 1 and Fig. 2c). Such a spread in interaction frequencies can be due either to a time dependent fluctuation of the EFG and/or to a static distribution of EFG values due to a spread in possible environments of the Cd probe. Although it is difficult to rule out the latter, in view of the facts that the interaction frequencies show a Lorentz distribution and the relaxation time is strongly temperature dependent (which would be hard to imagine for a static distribution), we conclude that the observed damping is caused by a dynamic fluctuation of the EFG at the Cd site. A large τ_N at high temperatures means that all probe nuclei feel quite similar environments: the EFG fluctuations are fast enough to nearly average out over the life time of probe. At low temperature, the spread in interaction frequencies appears to be much larger: slower EFG fluctuations cause that every probe nucleus becomes sensitive to the details of the local fluctuation history. The temperature variation of τ_N , summarized in Table II, could be fitted by the relation

$$\tau_N(T) = \tau_N(0)(1 + BT^\beta)$$

with $\tau_N(0) = 71$ ns and $\beta = 1.85$, revealing a nearly quadratic dependence.

How can we explain these three experimental observations? A straightforward suggestion to explain a fluctuating EFG with non-zero η would be to assume migration of Cd to other sites of lower symmetry and/or hopping/diffusion of oxygen from the CdO_6 octahedron. The former, however, is unlikely because in Sr_2RuO_4 the only substitutional site without axial symmetry is O(1) and it is highly improbable that Cd will replace an O-atom when chemically similar atoms as Sr and Ru are present. For the same reason, the occupation of an interstitial site is unlikely. Furthermore, in the case of site migration (diffusive/hopping motion) it is generally observed that the $\tau_N(T)$ shows an activation type (Arrhenius) behaviour²¹ in contrast to the power law dependence observed in the present case. Another way to explain the appearance of a non-zero η would be to invoke a long-range (e.g. Jahn-Teller like) lattice distortion. This possibility is excluded, however, by structural studies using high-resolution X-ray as well as neutron diffraction techniques.^{9,10,11} Both have failed to detect any lattice transformation or distortion in Sr_2RuO_4 down to 100 mK. As a result, only *short ranged* lattice distortions are allowed. In order to account for the fluctuations we have observed from the EFG, these distortions must also be *dynamic*. Our TDPAC results thus provide clear signatures of a dynamic lattice distortion in Sr_2RuO_4 below 300 K. The dynamic lattice distortion observed from our TDPAC measurements are consistent with the structural instability reported from phonon dispersion results observed by inelastic neutron scattering,¹² although there are subtle differences with respect to the temperature dependence. For instance, we observe that above 300 K these symmetry-breaking lattice distortions are varying fast enough to be averaged out over the time-window of our experiment (100-200 ns).

What could be the physical origin of the dynamic lattice distortions in Sr_2RuO_4 , observed through our TDPAC experiments? It is now well established that the highly correlated material Sr_2RuO_4 lies close to a magnetic instability.^{7,8} Recently, Fang and Terakura⁷ showed by first principle calculations based on the local spin density approximation (LDA) that the type of magnetic structure of Sr_2RuO_4 strongly influences its lattice structure. More precisely, the magnetic order influences the details of the RO_6 octahedrons (their tilt (θ), their rotation (ϕ) and their flatness λ , the latter defined as the ratio of the Ru-O bond length along the c-direction and along the a- or b-direction ($\lambda = d_c/d_{ab}$)). For the experimentally observed stable structure of Sr_2RuO_4 the ground state was found to be ferromagnetic, but non-magnetic and antiferromagnetic solutions with very small differences in total energy were found as well. Their calculated results revealed that Sr_2RuO_4 can be easily driven into different magnetic states by a small distortion of the lattice, especially by modifying the RuO_6 octahedron. We apply this argument in the opposite way: if – for instance as a result of spin fluctuations – the local magnetic structure of Sr_2RuO_4 will change continuously, it

will be accompanied by a local and continuously varying distortion. This gives rise both to the fluctuating EFG and the deviation from cubic symmetry. As these dynamic distortions are mediated by magnetic effects (spin fluctuations), they differ from the usual lattice dynamics. As a consequence, it is not surprising that we observe an anomalous temperature dependence of the EFG. At the lowest studied temperatures, the spin fluctuations are slow enough to provide every Cd probe with different sequence of fluctuations during its life time, leading to a large spread in observed interaction frequencies. Near room temperature, the spin fluctuations (and therefore the dynamic lattice distortions as well) are so fast that they average out over the relevant time window, and an averaged, axially symmetric environment is detected. Such short-ranged and time dependent lattice distortions can not be detected through X-ray or neutron diffraction experiments, which measure the long range correlation of atomic arrangements in solids, averaged over large time intervals and therefore insensitive to dynamic changes over short length scales. On the other hand, as demonstrated here, the affects of short range dynamic lattice modifications can manifest themselves in experiments by microscopic techniques such as TDPAC.

Further support for our interpretation of short-ranged dynamic lattice changes triggered by spin fluctuations comes from a series of *ab initio* calculations. We calculated the main component V_{zz} of the electric field gradient tensor for Cd in Sr_2RuO_4 , using a super cell to mimic the condition of an isolated impurity. The presence of a Cd impurity influences the positions of its neighboring Sr, Ru and O atoms, and we allowed the first three shells of Cd-neighbours (twice O and once Ru) to move to their new equilibrium positions. More distant neighbours hardly moved. Tests with different sizes of supercells showed that it was necessary to take a cell with 1 Cd atom per 16 formula units of Sr_2RuO_4 ($2\sqrt{2} \times 2\sqrt{2} \times 1$ supercell, containing 112 atoms). In such a supercell, the Cd atoms occupy a tetragonal (but nearly cubic) sublattice with Cd-Cd separations of 11.0 Å and 12.9 Å which is reassuringly large so that impurity-impurity interactions can be neglected³¹. The results obtained from these calculations, both for the unrelaxed (all atoms at ideal I4/mmm lattice sites) and the relaxed conditions are summarized in Table III. It must be mentioned that the lattice relaxations used in our calculations are only approximate as it was performed in a supercell with 1 Cd atom per 8 formula units, and the distances were carried over to the larger supercell. Calculating relaxations directly in the largest supercell was computationally too expensive.

If no spin-polarization nor lattice relaxation is allowed, the main component of the EFG tensor at a Cd impurity substituting Ru is calculated to be $V_{zz} = 2.2 \cdot 10^{21} \text{ V/m}^2$ (Tab. III). Including lattice relaxation, the EFG decreases to $V_{zz} = 1.1 \cdot 10^{21} \text{ V/m}^2$. Both these values are smaller compared to the range of experimental values observed in the temperature interval 20–500 K. The EFG

TABLE III: V_{zz} (10^{21} V/m^2) for a Cd impurity at the Ru position in unrelaxed and relaxed supercells with 16 formula units of Sr_2RuO_4 per Cd, for non-magnetic and antiferromagnetic calculations. The range of experimental values cover the interval 0 K – 500 K (see Fig 2).

	non-magnetic	AF	FM
V_{zz} / η Cd (unrelaxed)	2.2/0.00	1.9/0.09	1.5/0.00
V_{zz} / η Cd (relaxed)	1.1/0.00	4.2/0.01	4.5/0.00
V_{zz} / η Cd (exp)	4.3 – 5.5 / 0.0 – 0.3		

tensor is in both cases axially symmetric ($\eta = 0$), due to the point group symmetry at the Ru site. For the spin-polarized calculations, we tried two different spin configurations: antiferromagnetic (AF) and ferromagnetic (FM). Without lattice relaxations, the value of V_{zz} gets somewhat smaller compared to the non-magnetic case. It becomes considerably larger, however, if lattice relaxations are allowed: the magnetism does not affect the EFG directly, but it affects the lattice relaxation, which in turn affects the EFG. Most importantly, the order of magnitude (4.2-4.5) of V_{zz} is now perfectly comparable to the experimental observation (4.2 when extrapolated to 0 K). This corroborates our assumption that Cd indeed substitutes a Ru atom. If the applied spin configuration lacks axial symmetry (as is the case for our AF configuration, and as will be the case for any ‘random’ spin configuration that is the momentaneous result of fluctuating spins), the calculations show a non-zero η does indeed appear. The calculated values of 0.09 and 0.01 are smaller than the observed maximum of 0.30, but these values are for one particular AF configuration only. Taken all together, these *ab initio* calculations demonstrate that different spin configuration (as they appear during the spin fluctuation process) do indeed influence the EFG tensor at the Cd site, and lead to better numerical agreement between the calculated and measured EFG tensor.

In summary, by studying the quadrupole interaction of ^{111}Cd using the TDPAC technique and *ab initio* calculations, we have found evidence for a dynamic lattice distortion in Sr_2RuO_4 reflected by a rapidly fluctuating electric field gradient (EFG) and a temperature dependent change of its asymmetry parameter (η). The results presented in this work might contribute to understanding the mechanism of superconductivity in Sr_2RuO_4 .

Acknowledgments

Part of this work has been financially supported by Project No. G.0237.05 of the Fonds voor Wetenschappelijk Onderzoek – Vlaanderen (FWO), the Concerted Action Programme of the K.U.Leuven (GOA/2004/02), the Centers of Excellence Programme of the K.U.Leuven

(INPAC, EF/05/005) and the Inter-University Attraction Pole Programme (IUAP P5/1).

-
- * Electronic address: mishra@tifr.res.in
 † Electronic address: Stefaan.Cottenier@fys.kuleuven.be
- ¹ Y. Maeno, H. Hashimoto, K. Yoshida, S. Nishizaki, T. Fujita, J.G. Bednorz and F. Lichtenberg, *Nature (London)* **372**, 532 (1994);
 - ² Andrew Peter Mackenzie and Y. Maeno, *Rev. Mod. Phys.*, **75**, 657 (2003).
 - ³ Y. Maeno et. al., *J. Phys. Soc. Jpn.*, **66**, 1405 (1997).
 - ⁴ S. Nakatsuji, D. Hall, L. Balicas, Z. Fisk, K. Sugahara, M. Yoshioka and Y. Maeno, *Phys. Rev. Lett.*, **90**, 137202 (2003).
 - ⁵ T. Imai, A.W. Hunt, K.R. Thurber and F.C. Chou, *Phys. Rev. Lett.*, **81**, 3006 (1998).
 - ⁶ T. M. Rice and M. Sigrist, *J. Phys. Condens. Matter* **7**, L643 (1995); D.F. Agterberg, T.M. Rice and M. Sigrist, *Phys. Rev. Lett.*, **78**, 3374 (1997).
 - ⁷ Z. Fang and K. Terakura, *Phys. Rev. B* **64**, 020509(R) (2001).
 - ⁸ I.I. Mazin and D.J. Singh, *Phys. Rev. Lett.* **79**, 733 (1997); *Phys. Rev. Lett.* **82**, 4324 (1999).
 - ⁹ J.S. Gardner, G. Balakrishnan and D. McK. Paul, *Physica C* **265**, 251 (1996).
 - ¹⁰ T. Vogt and D.J. Buttrey, *Phys. Rev. B* **52**, R9843 (1995).
 - ¹¹ J.J. Neumeier, M.F. Hundley, M.G. Smith, J.D. Thompson, C. Allgeier, H. Xie, W. Yelon and J.S. Kim, *Phys. Rev. B* **50**, 17910 (1994).
 - ¹² M. Braden, W. Reichardt, S. Nishizaki, Y. Mori and Y. Maeno, *Phys. Rev. B* **57**, 1236 (1998).
 - ¹³ H. Mukuda, K. Ishida, Y. Kitaoka, K. Asayama, Z. Mao, Y. Mori and Y. Maeno, *J. Phys. Soc. Jap.*, **67**, 3945 (1998).
 - ¹⁴ K. Ishida, Y. Minami, Y. Kitaoka, S. Nakatsuji, N. Kikugawa and Y. Maeno, *Phys. Rev. B* **67**, 214412 (2003).
 - ¹⁵ K. Ishida, Y. Kitaoka, K. Asayama, S. Ikeda, S. Nishizaki, Y. Maeno, K. Yoshida and T. Fujita, *Phys. Rev. B* **56**, R505 (1997).
 - ¹⁶ G. Schatz and A. Weidinger, 1996 *Nuclear Condensed Matter Physics* (Wiley, New York).
 - ¹⁷ G.L. Catchen, T.M. Rearick and D.G. Schlom, *Phys. Rev. B* **49**, 318 (1994).
 - ¹⁸ P. Raghavan, 1989 *Atomic Data and Nuclear Data Tables* **42** 189-291.
 - ¹⁹ E. N. Kaufmann and R. J. Vianden, *Rev. Mod. Phys.* **51**, 161 (1979).
 - ²⁰ D. Torumba, K. Parlinski, M. Rots, and S. Cottenier, *Phys. Rev. B* **74**, 144304 (2006).
 - ²¹ E. B. Karlsson, *Solid State Phenomena as Seen by Muons, Protons and Excited Nuclei* (Clarendon Press, Oxford) 1995.
 - ²² P. Hohenberg and W. Kohn, *Phys. Rev.* **136**, 864 (1964).
 - ²³ W. Kohn and L.J. Sham, *Phys. Rev.* **140**, A1133 (1965).
 - ²⁴ S. Cottenier, "Density Functional Theory and the Family of (L)APW-methods: A Step-By-Step Introduction", Instituut voor Kern- en Stralingsfysica, KULeuven, Belgium, 2002, ISBN 90-807215-14.
 - ²⁵ E. Sjöstedt, L. Nordström and D.J. Singh, *Solid State Commun.* **114**, 15 (2000).
 - ²⁶ G. K. H. Madsen, P. Blaha, K. Schwarz, E. Sjöstedt, and L. Nordström, *Phys. Rev. B* **64**, 195134 (2001).
 - ²⁷ P. Blaha, K. Schwarz, G. Madsen, D. Kvasnicka and J. Luitz, "WIEN2k, an augmented plane wave + local orbitals program for calculating crystal properties", Karlheinz Schwarz, Techn. Universitat Wien, Austria, 1999, ISBN 3-9501031-1-2.
 - ²⁸ J. P. Perdew, K. Burke and M. Ernzerhof, *Phys. Rev. Lett.* **77**, 3865 (1996).
 - ²⁹ David J. Singh, *Phys. Rev. B* **52**, 1358 (1995).
 - ³⁰ Kiyoshi Betsuyaku and Hisatomo Harima, *Physica B* **284-288**, 1365 (2000).
 - ³¹ S. Cottenier, V. Bellini, M. Cakmak, F. Manghi and M. Rots, *Phys. Rev. B* **70** 155418 (2004).